Reducing biases in XBT measurements by including discrete information from pressure switches

Marlos Goes[1,2,*], Gustavo Goni[2], and Klaus Keller[3,4]

1 Cooperative Institute for Marine and Atmospheric Studies, University of Miami, Miami, FL, USA

2 Atlantic Oceanographic and Meteorological Laboratory, National Oceanic and Atmospheric Administration, Miami, FL, USA

3 Department of Geosciences, Penn State University, State College, PA, USA.

4 Earth and Environmental Systems Institute, State College, PA, USA.

Accepted in JTech – Final version

November 6, 2012

*Corresponding author: Marlos Goes, Cooperative Institute for Marine and Atmospheric Studies, Rosenstiel School of Marine and Atmospheric Science, University of Miami, 4600 Rickenbacker Causeway, Miami, FL, 33149, email: mgoes@rsmas.miami.edu and marlos.goes@noaa.gov .

Abstract:

Biases in the depth estimation of expendable bathythermograph (XBT) measurements cause considerable errors in oceanic estimates of climate variables. Efforts are currently underway to improve XBT probes by including pressure switches. Information from these pressure measurements can be used to minimize errors in the XBT depth estimation. Here we present a simple method to correct the XBT depth biases using a number of discrete pressure measurements. We use a blend of controlled simulations of XBT measurements and co-located XBT/CTD data along with statistical methods to estimate error parameters, and optimize the use of pressure switches in terms of number of switches, optimal depth detection, and errors in the pressure switch measurements to most efficiently correct XBT profiles. Our results show that given the typical XBT depth biases, using just two pressure switches is a reliable strategy for reducing depth errors, as it uses the least number of switches for an improved accuracy, and reduces the variance of the resulting correction. Using only one pressure switch efficiently corrects XBT depth errors when the surface depth offset is small, its optimal location is at mid-depth (around or below 300 m), and the pressure switch measurement errors are insignificant. If two pressure switches are used, results indicate that the measurements should be taken in the lower thermocline and deeper in the profile, at approximately 80 m and 600 m, respectively, with a RMSE of approximately 1.6 m for pressure errors of 1 m.

1. Introduction

The use of expendable bathythermograph (XBT) measurements started in the 1960's and rapidly became a preferred observational device for measuring upper ocean temperatures due to their ease of deployment and low cost, outnumbering the mechanical bathythermographs (MBTs) in the 1970's and the Conductivity-Temperature-Depth (CTD) in the 1990's (Gouretski and Koltermann, 2007). XBT observations account for a large percentage of the existing global ocean temperature record (Ishii and Kimoto, 2009), and are likely to still be utilized for many decades, despite the emergence of newer oceanic observing technologies.

The XBT probe has a streamlined body, comprised of a heavy metal nose, plastic triangular fins and a wire spool. When the XBT is dropped from a vessel, water flows past a thermistor through a cylindrical hole in the nose. The water temperature changes the thermistor resistance, producing a voltage response, which is captured on board the vessel and translated into a temperature measurement (Georgi et al., 1980; Green, 1984). Since the XBT probe does not contain pressure sensors, its depth estimate relies on a semi-empirical quadratic relationship between time of descent and depth, known as the fall rate equation (FRE):

$$Z = at - bt^2, \qquad (1)$$

which converts the time elapsed t (in seconds) since the probe hits the water to a depth Z (in meters). The FRE depends on two parameters, *a* and *b*, which account for the characteristics of the probe, as well as of the environment (Hallock and Teague, 1992; Green, 1984). According to the manufacturer (see Hanawa et al., 1994), the maximum tolerance for systematic errors associated with these depth estimates are typically ± 2% of depth linear bias, a depth offset of ± 5 m, and a temperature accuracy of ± 0.2^{o}C.

Recent studies (e.g., Wijffels et al., 2008) have shown that, for the historical XBT record, the magnitude of the depth error could be greater than 3% at 800 m, and that these errors may be dependent on the probe type and manufacturing year (Wijffels et al., 2008; Ishii and Kimoto, 2009; Gouretski and Reseghetti, 2010; Gouretski, 2012). Positive temperature biases are found in both MBT and XBT temperature measurements, but XBT biases may account for most of the apparent interannual variation of heat content in the ocean (Gouretski and Koltermann, 2007). This greatly affects the reliability of climate models in simulating the effect of heat uptake by the ocean, and, as a result, affects climate projections (e.g., Forest et al., 2002; Urban and Keller, 2009; Olson et al., 2012).

As a comparison, typical CTD measurements (e.g., Sea-Bird SBE 911) have a nominal accuracy of 0.001 °C, and a nominal depth resolution of 0.015 m. Despite the fact that such values are given for ideal conditions, and that the actual CTD precision may vary (see Boyer et al., 2011), CTD measurements are perhaps the best standard for a "true" temperature record. Several studies have analyzed the temperature errors of XBTs by comparing XBT measurements with co-located CTD measurements (e.g., Flierl and Robinson, 1977; Heinmiller, et al., 1983; Hallock and Teague, 1991; Kizu and Hanawa, 2002; Reseghetti et al., 2007). Historically, the temperature gradient method has been the most widely used. By comparing the temperature gradients with depth (dT/dz) of a CTD profile with those from an XBT profile, the XBT depth bias can be corrected by finding vertical lags of maximum correlation and estimating stretching terms to be applied to the XBT depth (Hanawa and Yoritaka, 1987; Hanawa and Yasuda, 1992). Other methodologies have also been successfully applied for XBT profiles correction, such as the technique proposed by Cheng et al. (2011), where the integral temperature instead of the temperature gradient seems to improve on the temperature gradient method considerably.

Moreover, such a technique intrinsically requires an offset depth term. True thermal biases in XBTs may also be estimated after the depth correction (DiNezio and Goni, 2011, Cowley et al., 2012), but this also requires information from a co-located CTD profile along the entire depth of the XBT profile. Results from previous studies (e.g., Levitus et al., 2009, Gouretski and Reseghetti, 2010) indicate that thermal biases were generally higher, between 0.1-0.2°C from the 60's through the 80's, and decreased later on, stabilizing after 2000 at around 0.05°C.
The FRE is highly dependent on many parameters, such as the viscosity of the water, the height of the launch, and the state of the ocean where the probes are deployed. Parametric uncertainty in the FRE is the biggest contributor for temperature biases in XBT measurements. Supplementary information could be used to constrain the XBT depth estimates: for instance, the addition of pressure switches inside the probe could potentially reduce depth biases without a considerable price increase. Pressure switches are small resistors that are activated at certain depths during the probe descent, marking those depths in the profile with spikes. These spikes are filtered during post processing, and their depths are recorded and used to correct depth biases in the profile.

Here, our goal is to investigate if future measurements from pressure switches will be able to appropriately correct XBT depth biases. To this end, we derive an efficient and practical approach that improves on current methodologies by not requiring the use of collocated CTD profiles.

This manuscript is outlined as follows. In Section 2 we define the two datasets used in this study. In Section 3 we derive the methodology for the correction of the XBT depth biases using pressure switches, and the two statistical methods used to optimize the correction. In Section 4, we use simulated temperature profiles to test the capability of this correction with respect to (i) the number of switches and (ii) the errors in the pressure switch measurements. Additionally, we use co-located temperature profiles to test the capability of the method on actual data, and (iii) estimate the optimal depths for triggering the switches. Finally, in Section 5 we discuss the main results of this study, including advantages and caveats of using pressure switches.

2. Data

We use two types of data in the present study: (a) climatological temperature profiles, and (b) shipboard co-located temperature XBT/CTD profiles. These two datasets and their application in the present study can be described as follows:

a) The experiments with simulated data are based on typical temperature profiles from the World Ocean Atlas climatology product (WOA09; Locarnini et al., 2009), which consist of gridded data with a 5^o x 5^o horizontal resolution and 27 vertical levels. For the purpose of this study, we use data from the upper 700 m of the ocean, interpolated linearly onto a 10 m vertical resolution.

b) The experiment with co-located data uses XBT and CTD observations collected in the tropical North Atlantic during the PIRATA Northeast Extension 2009 (PNE09) cruise (DiNezio and Goni, 2011). We selected 19 paired XBT and CTD casts deployed within 24 hours and ~10 km apart. The selected XBT probes are the Sippican T7 manufactured in 1986, which are the probes that showed the highest overall depth error in this dataset (DiNezio and Goni, 2011). The original Sippican FRE coefficients ($a = 6.472$ m s^{-1} and $b = 216 \times 10^{-5}$ m s^{-2}) are used to estimate the XBT depth (Z_{XBT}).

3. Methodology

3.1 Errors in XBT measurements

Simultaneous XBT-CTD experiments (e.g., Flierl and Robinson, 1977; Hanawa, 1995; Thadathil et al., 2002) have shown that the manufacturer FRE parameterization may be inadequate to produce unbiased temperature data in the upper ocean. We illustrate the effect of an inaccurate FRE parameterization on the 0-700 m global ocean heat content anomaly (OHCA) by simulating a linear depth bias time variability as a sinusoidal with amplitude of 2% of depth (Figure 1). OHCA is calculated globally using the WOA09 annual climatology (see Section 2a for data description), and assuming that 50% of the global profiles are randomly affected by a common depth bias. The global effect of the XBT depth biases in this simulation generates OHCAs with amplitude on the order of 8 x 10^{22} J, which is the same order of magnitude as the observed global OHCA linear trends since the 1960's calculated in Domingues et al. 2008 (~16 x 10^{22} J) and in other recent studies (e.g., Levitus et al., 2009; Ishii and Kimoto, 2009), therefore complicating the detection of human induced trends in ocean heat uptake.

In general, XBT-derived temperature profiles are affected by several sources of error (see for example, Cheng et al., 2011). We have chosen to focus on four sources of errors in our analysis:

1) Pure temperature errors (T_0): These are remaining temperature errors after XBT depth correction. These errors can be introduced by several factors, including probe-to-recording device, (static) calibrations in laboratory, wire de-reeling, and leakages, most of which producing a positive temperature bias (Cook and Sy, 2000; Reseghetti et al., 2007; Gouretski and Reseghetti, 2010). The manufacturer temperature error is on the order of 0.2°C (Hallock and Teague, 1992; Ishii and Kimoto, 2009, Gouretski and Reseguetti, 2009), and we use this value as a constant temperature offset.
2) Inaccurate FRE parameterization (z_d, z_2): This is the pure FRE error. z_d is defined as a linear depth bias given as a percentage of depth (Seaver and Kuleshov, 1982). We use z_d

= 3% of depth as a typical value of this parameter, which is in agreement with previous studies (e.g., Wijffels et al., 2008), and slightly higher than the manufacturer specification of 2%. z_2 is a quadratic bias term, and is related to an acceleration term in the FRE (Cowley et al., 2012). We consider this term $z_2 = 1e^{-5}\ m^{-1}$, which alone generates an error of ~ 5 m at 700 m depth, and is in agreement with the estimates of Hamon et al. (2011) and Cowley et al. (2012).

3) Depth bias (z_0): This error arises from surface phenomena such as wave height variability, entry velocity and angle of the probe (e.g., Abraham et al., 2012). In this manuscript we use z_0 as a constant depth offset, typically z_0 = 5 m (Gouretski and Reseghetti, 2010).

4) Random errors (ε_z, ε_T, ε_p): These errors affect all measurements, due to small variations in the mean state of the environment, and also to the precision of individual probes (Georgi et al., 1980). Here we approximate the random errors by a Gaussian distribution $N(0, \sigma_i^2)$ with mean zero and standard deviation σ_i. We distinguish three types of random errors, for depth (ε_z), temperature (ε_T), and pressure (ε_p).

The typical values of the parameters used here are summarized in Table 1. Formally, we treat the four classes of XBT errors described above as deviations from an "error-free profile", which represents a CTD profile. Therefore, the depth of the XBT profile (Z_{XBT}) is the depth of the error-free CTD profile (Z_{CTD}) plus the total depth errors (E_Z):

$$Z_{XBT} = Z_{CTD} + E_Z\ , \qquad (2a)$$

and the total temperature errors in XBT measurements (E_T) are defined similarly:

$$T_{XBT} = T_{CTD} + E_T\ , \qquad (2b)$$

where T_{XBT} and T_{CTD} are the XBT and the error-free temperature profiles, respectively.

The error components E_z and E_T are structured as follows:

$$E_Z = z_0 + z_d Z_{CTD} + z_2 Z_{CTD}^2 + \varepsilon_Z \quad (3a)$$

$$E_T = T_0 + \varepsilon_T \ . \quad (3b)$$

In simulating discrete pressure switch measurements, additional contributions to the total errors arise from random errors (ε_p) in the pressure measurements themselves. Therefore, a certain pressure measurement P is decomposed as:

$$P = P_{CTD} + \varepsilon_p \ . \quad (4)$$

3.2 Correction of the XBT measurement biases using pressure switches

Having defined the XBT errors analytically, we now derive a correction to the XBT profile using pressure switch information. This correction is performed in two steps, (1) by first identifying the errors E_Z and E_T in equation (3a, b) and (2) subtracting them from the profiles. For this, we assume that *n* pressure switch measurements (P_n) are performed during the descent of the XBT probe through the water column (Figure 2), and the locations of these measurements ($Z(P_n)$) provide information about the correct depth of the profile. The correct depth of the XBT profile (Z_{CORR}) is then given by an operational fall rate equation estimate (Z_{XBT}) minus a depth correction *F* which is a function of the pressure measurements:

$$Z_{CORR} = Z_{XBT} - F(Z(P_n)) \ . \quad (5)$$

Equation (5) is a continuous function of depth, but in practice it relies only on the discrete locations of the pressure measurements. Using equations (2a) and (5), we derive the function F at the *n* discrete locations as:

$$F(Z(P_n)) = (Z_{XBT_n} - Z(P_n)) = z_0 + z_d Z(P_n) + z_2 Z^2(P_n)\,. \quad (6)$$

The reconstruction of the entire corrected profile depth (Z_{CORR}), which is known at discrete locations $Z(P_n)$, is performed by isolating $Z(P_n)$ from the second and third terms in equation (6), making it dependent on Z_{XBT} and the error parameters.

The degrees of freedom of the correction are determined by the number of pressure switches to be used. For $n \leq 2$ switches and/or when the quadratic term (z_2) in Equation (6) is ignored, we apply a linear correction. For $n \geq 3$ and $z_2 \neq 0$, we use a quadratic correction.

Z_{CORR} is calculated as follows:

(i) Linear correction ($n \leq 2$ switches or $z_2 = 0$): Solving the linear version of equation (6), we have:

$$Z_{CORR} \approx Z(P_n) = \frac{Z_{XBT}}{1+z_d} - \frac{z_0}{1+z_d}\,. \quad (7)$$

This approach is considered an unbiased estimator for quasi-linear errors and accurate pressure measurements. If only one pressure switch ($n = 1$) is installed in the XBT probe, we assume that $P_1 = P_{XBT_1}$, i.e., the pressure estimated at the initial depth of the XBT profile P_{XBT_1} is measured by a virtual pressure switch at the surface for calculation of the correction terms.

(ii) Quadratic correction ($n \geq 3$ switches and $z_2 \neq 0$): The quadratic version of equation (6) produces a corrected depth according to:

$$Z_{CORR} \approx Z(P_n) = \frac{-(1+z_d) + \sqrt{(1+z_d)^2 + 4z_2(Z_{XBT} - z_0)}}{2z_2}, \qquad (8)$$

which takes into account only the positive sign of the square root to allow compensation between the two terms on the right side of Equation (8), and therefore limiting to a finite root value for small values of z_2.

Note that for the approaches (i) and (ii) to be applied, depth is first converted to pressure to simulate the pressure switch measurements, and later the corrected pressure profile is converted back to depth. We adopt the Saunders (1981) algorithm for the conversion between depth and pressure, which does not account for temperature and salinity effects on the pressure in the water column, and presents an average error of 0.1 m. For a number of *n* pressure switches, the parameters z_0, z_d and z_2 are calculated using a least squares regression with *n* points.

After the depth correction, the pure temperature bias can be determined by the average residual temperature in the profile:

$$T_0 = \frac{\sum_{k=1}^{K} (T_{XBT}^k - T_{CTD}^k)}{K}. \qquad (9)$$

As in previous studies (e.g., Flierl and Robinson, 1977; Gouretski and Reseghetti, 2010), equation (9) can only be applied to collocated temperature profiles.

3.3 Optimization methods for determining switch number and location

The method described in Section 3.2 applies for *n* pressure switches. The estimation of the number of switches and the depths at which they are triggered during the probe descent is an optimization problem. We use two optimization methods: (a) a "brute force" Root Mean Square Error (RMSE) minimization is applied to simulated profiles as a sensitivity test for different number of pressure switches and different sets of errors, and (b) a global optimization algorithm for a likelihood maximization is applied to co-located XBT/CTD data to determine the triggering depth of the pressure switches.

a) RMSE minimization of simulated data

These idealized experiments use simulated profiles based on the temperature profiles from the WOA09 annual climatology. The original climatological profiles are considered error-free CTD observations, whereas the XBT observations are simulated by adding typical errors to the original profiles. We simulate measurements of one to five pressure switches distributed randomly along the XBT profile, and analyze three different cases, each of them using a different set of errors in the simulated XBT profiles. In order to sample a large number of possible combinations of the pressure switch locations, we select 12,500 random realizations of the positions of the switches and random errors.

The accuracy of the FRE correction by pressure switch measurements is evaluated at a given combination of location of pressure switches using the root mean square error (RMSE), defined as:

$$RMSE = \sqrt{\frac{\sum_{k=1}^{K}(Z_{CORR}^{k} - Z_{CTD}^{k})^2}{K}}, \quad (10)$$

In the RMSE calculation, the temperature of the corrected profile is linearly interpolated to the depth of the original error-free profile. The RMSE is used to represent the goodness of fit between the CTD and the corrected XBT profile at each set of locations. The minimum RMSE value provides the optimal locations of the switches. In the case of generating repeated locations, we take the median value of the RMSE and derived error parameters to represent these locations.

b) The maximum likelihood method for shipboard co-located data

The RMSE method described in (a) requires relatively expensive computation, neglects residual auto-correlation, and does not consider the error parameters simultaneously. Here we introduce a global optimization method to estimate simultaneously the mismatches between XBT/CTD co-located data (Section 2b). The optimization is performed using the dynamical evolution method (Storn and Price, 1997), an efficient method for sampling possible values of a parameter space θ and accounts for multimodality. This statistical model assumes that the temperature differences between the CTD and XBT observations are randomly distributed and auto-correlated.

According to equations (2b) and (3b), the temperature residual error is a random variable drawn from a multivariate normal distribution

$$E_T \sim N(T_0, \Sigma), \tag{11}$$

with an unknown mean temperature or offset term T_0, and a covariance matrix Σ, approximated by the residual variance $\sigma_T{}^2$ multiplied by an auto-correlation that decays exponentially between two depths Z_j and Z_k with a length scale λ:

$$\Sigma_{jk} = \sigma_T^2 \exp(-\left|Z_j - Z_k\right| / \lambda) \ . \tag{12}$$

We estimate simultaneously up to nine parameters θ = (T_0, z_0, z_d, z_2, λ, σ_T, $Z(P_1)$, $Z(P_2)$, $Z(P_3)$), which are the XBT errors plus the optimal depths of the pressure switches. Out of these nine estimated parameters, six are estimated simultaneously. z_0, z_d and z_2 are estimated separately, since they are derivative parameters calculated during the correction. The optimal values of these parameters are calculated by maximizing a Gaussian likelihood objective function $L(T \mid \theta)$ given for the temperature data conditional on the error parameters θ:

$$L(T \mid \theta) \propto \exp\left(-\frac{(\Delta T^{T} \Sigma^{-1} \Delta T)}{2}\right), \qquad (13)$$

where $\Delta T = (T_{XBT} - T_0) - T_{CTD}$ is the residual temperature, which accounts explicitly for the temperature bias term T_0, and T_{XBT} is defined at the corrected depth Z_{CORR}, linearly interpolated to Z_{CTD}.

4. Results

We test the effectiveness of the pressure switch correction of simulated XBT profiles in three idealized experiments, using as base different climatological temperature profiles and sets of errors. As a first test, we validate the method to assure that it is capable of estimating the XBT error parameters

4.1 Simulated profiles

To assess whether our approach is an unbiased estimator of the error parameters of an XBT profile, we perform a simple experiment using a simulated profile. For an unbiased estimator, the mean of the sampling distribution of one estimated parameter must be equal to the true value of the parameter. In this experiment, the simulated XBT profile contains all typical errors (Table 1), and the steps described in Section 3.2 are followed in order to estimate the error parameters. Thus a linear version the correction approach is applied for $n \leq 2$, and a quadratic version for $n \geq 3$. The residual errors (XBT minus CTD) are estimated using information from one to five switches placed along the XBT temperature profile. A comparison between the error histograms estimated from the 12,500 realizations of the corrections using $n = 1$ to $n = 5$ pressure switches and the original input errors used to simulate the XBT profile are shown in Figure 3. The largest discrepancies are observed for the error estimates using only one switch ($n = 1$). In particular the depth offset is poorly resolved, showing median values of -0.4 m, instead of the input value of $z_0 = 5$ m. The histograms of z_d and T_0 exhibit a long tail, showing that in this case the determination of the depth errors is subject to high uncertainty. For $n = 2$, T_0 and z_0 are precisely estimated, and z_d is within the 60th percentile, but the median is located slightly above the correct value of $z_d = 3.6$ m, to compensate for the missing quadratic term. For $n \geq 3$, there is a good agreement between the input and estimated errors in most of the realizations of pressure switch locations, confirming that this methodology is a potentially unbiased estimator of the FRE errors. As we increase the number of switches, the peak of the parameters histogram is slightly sharpened, showing that in the case of a very dense number of switches the method reproduces the actual temperature profile almost perfectly.

4.1.1 Number of pressure switches

Next, we explore the sensitivity of the correction of the XBT depth estimate using pressure switches to different errors and different numbers of pressure switches. We simulate three XBT deployments, each of them subject to different sets of measurement errors. To illustrate how the depth errors affect different profiles, we use as base three WOA09 climatological profiles from a tropical region, which have the strongest gradients. Different outcomes will be produced by the correction, thus each case (named a, b and c) will be analyzed separately as itemized below.

a) (z_d, ε_z, ε_T, ε_p): In this experiment we apply only a linear depth bias and random errors into a tropical profile (Figure 4a). The median temperature residuals with respect to the CTD profile (Figure 4b) show an improvement achieved by the depth correction independent of the number of switches. The original XBT profile shows higher deviation from the CTD profile in the thermocline $\Delta T = 0.4°C$, where gradients are stronger. After the correction, temperature residuals are mostly negligible, centered at $\Delta T = 0°C$ along the whole profile. This is because the linear depth biases, which cause an error of ~20 m at 700 m depth, are the only cause of temperature errors in this simulated XBT profile, and these errors are efficiently reduced by a correction by any number of switches (Figure 4c). The depth RMSE of the corrected profiles is sensitive to the location of the switches (Figure 4d, e), mostly because of the applied random errors. Random errors affect the correction if the switches are placed relatively near each other, and the RMSE decreases for a deeper location of the deeper switches (Figure 4d). The median RMSE of the 12,500 realizations show low variability among the number of switches applied in the correction, ranging from 10^{-1} m < RMSE < 1 m, in comparison to RMSE ≈ 10 m for the uncorrected (n=0) XBT depth (Figure 4e). Therefore, the correction provides a great improvement in the RMSE for this set of errors towards the uncorrected XBT profile using any number of switches. The thickness of the box plots in Figure 4e provides information about the variance of the correction, and serves as an indicator for the optimal number of pressure switches. The more switches added in this linear approach reduces the variance of the correction by averaging the random errors.

b) (z_0, z_d, ε_z, ε_T, ε_p): Here we add to the previous set of errors a depth offset (z_0) to the simulated XBT profile (Figure 5a). Increased temperature errors of up to 1.3°C are observed along the thermocline around 100 m depth (Figure 5b). After correcting the XBT profile with one pressure switch (Figure 5b), there is still a noticeable residual temperature error of about 0.3°C in the thermocline. Indeed, the addition of the depth offset z_0 mostly affects the correction using one pressure switch. A residual linear depth bias remains after the correction using one switch (Figure 5c), with the linear form $E_z = 0.011*Z + 5.05$ m, which shows that z_d was reduced from 3% to ~1%, but $z_0 \approx 5$ m is still present in the corrected profile. Best results for one switch are achieved if the switch is located deeper in the water column, below 400 m (Figure 5d). In comparison to the integral error of the uncorrected XBT profile (RMSE = 17 m; Figure 5e), the correction with two or more switches in this linear approach can efficiently eliminate most this bias, reducing the error to a RMSE = 0.1 m. Inaccurate information about the surface pressure can bring very different outcomes to the one switch correction (Figure 5e), shown by the increased variance of this correction with respect to the experiment (a). This feature illustrates that the depth bias offset (Z_0) can have an important role in producing residual linear depth biases after the correction with one switch.

c) (T_0, z_0, z_d, z_2, ε_z, ε_T, ε_p): In this experiment we use an additional quadratic term (z_2) in the FRE bias, as described in equation (8). For this $z_2 = 1e^{-5}$ m^{-1}, which agrees with recent estimates (Hamon et al., 2011). This bias term represents an acceleration term, which appears in some XBT measurements caused by the probe adjustment to the terminal velocity (Cowley et al., 2012). We use this experiment to contrast the linear versus the quadratic fit of the equation (5), in the presence of a quadratic depth error. The linear fit is used for the correction with one and two switches, and the quadratic fit is used for three or more switches, because more than three switches support the degrees of freedom necessary for the quadratic regression. We explore the results using a tropical profile (Figure 6a).

In this experiment we also add a temperature offset T_0 and analyze how T_0 can be detected after the depth correction. Results from this experiment show that one switch cannot detect the temperature offset well (Figure 6b), since there are still strong depth errors associated to the corrected profiles. Surprisingly, two switches are able to detect reasonably well the thermal offset of T_0 = 0.2°C after the correction (Figure 6b), a result similar to the correction with three switches.

Three or more switches can reduce the depth biases to nearly zero in the whole water column (Figure 6c). However, because the quadratic fit has more degrees of freedom, three switches show a high variance in comparison to the two switches case (Figure 6e). More than four switches can restrict the variance of the quadratic fit given the simulated measurement errors.

The linear fit used for two switches can also constrain the depth bias in most of the profile (Figure 6c). In the bottom of the profile errors are on order of 2 m, but the median of the residual error (RMSE < 1m) is similar to the RMSE after the quadratic correction using three switches (Figure 6e), showing that a linear approach can still reasonably correct profiles with typical acceleration biases of $z_2 \approx 1e^{-5}$ m^{-1}. Additional simulations (not shown) with increased acceleration bias ($z_2 > 1e^{-4}$ m^{-1}) show that the linear fit cannot constrain these errors, and the RMSE increases to about 10 m.

4.1.2 Errors in the pressure measurement

The accuracy of the depth correction is dependent on the accuracy of the pressure switch measurements. The accuracy of the pressure switches is greatly dependent on the quality of the equipment. Manufacturing costs of the pressure switches have to be considered when producing such equipment to achieve the best performance at the lowest possible cost. Therefore, it is crucial to assess how errors in pressure switch measurements can affect the accuracy of the correction, and what is their acceptable range.

Current technology is available to make this task relatively easy and inexpensive. This technology will allow including discrete pressure measurements with accuracy of 0.85 m to 1 m (Sippican, personal contact). Therefore we use p_0 = 1m as a threshold for the pressure switch accuracy in the present experiment, and estimate the depth RMSE after the correction with *n* switches.

Following the same methodology of the previous subsection, we use a simulated profile with typical XBT errors (Table 1), draw 12,500 random realizations of the location of the pressure switches, and analyze the residual biases after correcting the profile with these measurements. In addition to the precision errors, which are approximated by Gaussian random errors $\varepsilon_p = N(0,\sigma_p^2)$ with σ_p = 0.1 m in equation (4), we include a pressure offset term (p_0) varying between 0 and 5 m in 0.2 m increments. Equation 4 therefore becomes:

$$P = P_{CTD} + p_0 + \varepsilon_p \, . \qquad (14)$$

The median of the distribution of the RMSE of the 12,500 realizations as a function of the random errors and number of pressure switches is shown in Figure 7. For small pressure errors (p_0 < 2 m), there is a large gain of accuracy in going from one switch to two switches, but not much improvement is gained when more pressure switches are added. At higher pressure errors, the corrections with one and two switches show similar RMSE, when $p_0 \approx z_0$, since z_0 is the error inherent to the surface measurement using one switch correction. Accuracy is improved by adding more than two switches, which averages the random errors, as well as by using a quadratic correction instead of a linear, which improves the RMSE on the order of 0.5 m to 1 m for errors deep in the profile. Using p_0 = 1 m as a threshold, the RMSE = 1.6 m for two switches and RMSE = 1 m for three or more switches. One pressure switch gives an RMSE > 3 m for the considered threshold.

4.2 Correction of actual co-located CTD/XBT data

Here we test the ability of our approach in correcting XBT measurements biases using simultaneous CTD and XBT deployments. Results shown here are from 19 collocated CTD and XBT casts collected in the tropical Atlantic. This data have previously been analyzed by DiNezio and Goni (2011), which used the temperature gradient method to correct the XBT depth errors, and diagnosed the average errors among these profiles of z_d = 3.77 ± 0.57 % of depth, z_0 = 0.2 ± 1.54 m, and T_0 = -0.03 ± 0.17 °C. We compare our results with those from DiNezio and Goni (2011) as a validation for the present method. A comparison of the XBT profiles from other manufacturing years was also performed on this dataset, but not shown here, since it produced similar results. The profiles are smoothed with an 11 m triangular window to avoid spikes and interpolated to a 10 m vertical resolution. In this dataset, the XBT and the CTD data are available on the same vertical grid. Therefore, to simulate the pressure switch measurements, we interpolate the CTD data to the corrected XBT depth estimated by DiNezio and Goni (2011) using the temperature gradient method. This step generates undesirable noise, inherent from the gradient method, but is necessary to construct the pseudo-pressure observations.

The original XBT profiles (gray dots in Figure 8) show a cold bias with respect to the CTD profiles, evident as a median displacement to the left of about 0.2 °C in the temperature residuals

(Figure 8a, c, e). This is a joint effect of depth biases and thermal offset. In the thermocline, located around 70-80 m, the cold bias intensifies (< -1°C in some profiles), a feature that is also observed in the simulated profiles (Figures 4, 5 and 6). Depth differences of the original XBT profiles relative to the CTD profiles show linearly increasing biases at depths below 150 m (Figure 8 b, d, f), and are higher than 20 m at 700 m deep. Some outliers in the depth residuals arise because we use the temperature gradient method of DiNezio and Goni (2011) to estimate the CTD depths, as described in the beginning of this section, which is used to simulate the pressure switch measurements.

We apply the pressure switch correction using one, two and three switches, using the quadratic approach for three switches. The temperature biases after the correction are small, and most of the temperature biases in the original XBT profile are result of depth errors, therefore the temperature residuals after correction are mostly within the manufacturer's 0.2°C tolerance (colored dots in Figure 8a, c, e). Only in the correction with one pressure switch (Figure 8a) do considerable mismatches still remain within the thermocline, with a maximum up to 1°C. For two and three switches this maximum reduces to less than ~0.5°C. The depth biases after correction (Figure 8b, d, f) are also mostly contained within the manufacturer's limits, but the correction with one switch shows a much larger spread of the residuals than for two and three switches.

The statistical optimization (Section 3.3b) estimates simultaneously, and for each cast individually, the XBT measurement error and the optimal position of the switches to correct the depth errors. The distributions of these optimal parameters are shown in Figure 9, and summarized in Table 2 for the correction with one, two and three switches. The three corrections are capable of reducing the RMSE considerably from the uncorrected XBT (Figure 9f). The results show a median RMSE of ~3 m for the correction with one switch, and ~2 m for two and three switches, against 14 m in the uncorrected XBT.

There is a wide range of possible optimal locations of the pressure switches (Figure 9e), and particularly high variance is observed in the location for one pressure switch and for the deeper switch in the two switches correction. Since the distributions of the estimated values parameter are skewed (Figure 9), we use a bootstrap approach with 2000 samples to estimate the median and the standard deviation of the optimal depths of pressure switches. For one pressure switch the optimal position is at mid-depth, $Z(P_2) = 289 \pm 198$ m. For two switches the optimal positions are $Z(P_1) = 76 \pm 78$ m and $Z(P_2) = 593 \pm 168$ m, i.e., within the lower thermocline and deeper in the profile. Comparing the estimates of the XBT error parameters with the ones from DiNezio and Goni (2011), results show that all estimated parameters are within the previously estimated uncertainty. However, the one-switch correction estimates a negative median depth offset ($z_0 = -0.85$ m) in comparison to a positive value in the other two estimates ($z_0 = 0.20$ m).

5. Conclusions

In this study we present an approach for correcting XBT depth bias using a discrete number of pressure switch measurements. This approach can serve as a benchmark for the application of pressure switches to correct XBT temperature profiles. We test this approach on several experiments using tropical temperature profiles, by correcting simulated temperature profiles with known errors added, and also by correcting co-located XBT and CTD casts.

Results obtained here indicate that the efficiency of the XBT depth correction is generally sensitive to the number of pressure switches employed. Using only one pressure switch can result in a high variance in the efficacy of the correction because the depth offset cannot be estimated with one switch only. A good improvement towards reducing depth errors is achieved if the depth offset is absent or small, and the best quality of the depth correction can be achieved if the switch is triggered around 300 m or deeper. The two pressure switches strategy shows the best tradeoff between the reduction of the XBT depth biases and the number of switches. It improves on the one switch strategy by producing a much reduced variance of outcomes with respect to the location of the switches, and a comparable RMSE to the correction with three switches. This result holds when we include typical quadratic errors ($z_2 \approx 1e^{-5}$ m^{-1}), which departs slightly from a linear case and produces a depth error of 5 m at 700m. Sensitivity tests show that for higher quadratic errors ($z_2 > 1e^{-4}$ m^{-1}), applying two pressure switches becomes are less efficient, producing an RMSE > 10 m. With three pressure switches, the correction improves slightly from the two switches case by averaging random errors when a linear approach is applied. Three switches are able to detect the quadratic depth errors using a quadratic approach, though their associated correction allows a high variance in a quadratic fit because of the low constraint for 2 degrees of freedom. Four or more switches can reduce random errors and decrease the variance of a quadratic fit. Results from the collocated profiles in the tropical Atlantic yield optimal switching positions at mid-depth of Z(P1) = 289±198 m for one switch, and at the thermocline Z(P1) = 76±78 m and deep in the profile ($Z(P_2)$ = 593±168 m) for two switches.

By simulating variable accuracy in the pressure measurements, and accounting for typical random errors, we use a threshold of 1 m for the pressure switch accuracy to infer the typical

RMSE for the correction of quadratic depth errors. The correction using one pressure switch results in an RMSE > 3.5 m, for two switches an RMSE = 1.6 m, and for three or more switches an RMSE = 1 m.

According to the results shown here, the inclusion of pressure switches in XBT probes can be beneficial for scientific purposes, especially in climate studies, by reducing uncertainties in ocean heat content and sea level variability estimates. We expect our theoretical results to be validated in the tropical regions with real pressure switch measurements to be included in XBT prototype probes. Regional characteristics include changes in environmental properties of the water, such as kinematic viscosity, which is highly dependent on the temperature (Seaver and Kuleshov, 1982). Errors should vary geographically, following the local water temperature (Green, 1984; Hanawa, 1995; Thadathil et al., 2002), and the position of the switches could possibly vary too. We do not explicitly account for the latitudinal variability of errors.

Additional improvements on the XBT probe or comparisons with other temperature profiles are required to correct pure thermal biases. A thermal offset (typically $T_0 \approx 10^{-1}$ °C) may be caused, for example, by the recording system (e.g. Cowley et al., 2012), and the accuracy of the temperature measurement in comparison to a static calibration of the thermistor is limited by the high falling speed of XBT probes (at least, six times faster than the CTD). Comparing the depth corrected XBT with CTD profiles, or using an XBT tester probe (with fixed and well known resistances), for example, can provide quantification of the XBT thermal offset of the whole XBT system (probe + cable + recording system). New probes with improved thermistors and calibrations will aid to reduce temperature biases that would still remain after the depth biases correction.

Acknowledgements

The authors would like to thank Pedro DiNezio for interesting discussions and support with the collocated data, the PNE crew for collecting the collocated profiles, Chris Meinen and Libby Johns for revising the manuscript, and anonymous reviewers for greatly improving the final version of the manuscript. This research was carried out under the auspices of the Cooperative Institute for Marine and Atmospheric Studies (CIMAS), a cooperative institute of the University of Miami and the National Oceanic and Atmospheric Administration, cooperative agreement #NA17RJ1226, and was partly funded by the NOAA Climate Program Office.

References

Abraham, J. P., J. M. Gorman, F. Reseghetti, E. M. Sparrow, and W. J. Minkowycz, 2012: Drag coefficients for rotating expendable bathythermographs and the impact of launch parameters on depth predictions, *Num. Heat Transfer, Part A*, 62, 1, 25-43

Boyer, T., et al., 2011: Investigation of XBT and XCTD biases in the Arabian Sea and the Bay of Bengal with implications for climate studies, *J. Atmos. and Ocean. Tech*., 28, 266-286.

Cheng, L., J. Zhu, F. Reseghetti, Q. Liu, 2011: A new method to estimate the systematical biases of expendable bathythermograph, *J. Atmos. and Ocean. Tech*., 28, 2, 244-265.

Cook, S., and A. Sy, 2000: Best guide and principles manual for the Ships of Opportunity Program (SOOP) and eXpendable Bathythermograph (XBT) operations, Prepared for the IOC-WMO-3rd Session of the JCOMM Ship of Opportunity Implementation Panel (SOOPIP-III), March 28-31, 2000, La Jolla, California, USA, 1-26, 2001.

Cowley, R., S. Wijffels, L. Cheng, T. Boyer, S. Kizu, 2012: Biases in expendable bathythermograph data: a new view based on historical side-by-side comparisons, *J. Atmos. and Ocean. Tech*., submitted.

DiNezio, P., and G. Goni, 2011: Direct evidence of a changing fall-rate bias in XBTs manufactured during 1986-2008, *J. Atmos. and Ocean. Tech*., 28, 11, 1569-1578.

Domingues, C. M., J. A. Church, N. J. White, P. J. Gleckler, S. E. Wijffels, P. M. Barker, J. R. Dunn, 2008: Improved estimates of upper-ocean warming and multi-decadal sea-level rise, *Nature*, 453, 1090-1093, doi:10.1038/nature07080.

Flierl, G., and A. R. Robinson, 1977: XBT measurements of the thermal gradient in the MODE eddy, *J. Phys. Oceanogr*., 7, 300–302.

Forest, C. E., P. Stone, A. Sokolov, M. Allen, and M. Webster, 2002: Quantifying uncertainties in climate system properties with the use of recent climate observations, *Science*, 295 (5552), 113-117, doi:10.1126/science.1064419.

Georgi, D., T., J. P. Dean, and J. A. Chase, 1980: Temperature calibration of expendable bathythermographs, *Ocean Eng.*, 7(4), 491-499, doi: 10.1016/0029-8018(80)90048-7.

Gouretski, V., and K. P. Koltermann, 2007: How much is the ocean really warming?, *Geophys. Res. Lett*., 34, L01610, doi:10.1029/2006GL027834.

Gouretski, V., and F. Reseghetti, 2010: On depth and temperature biases in bathythermograph data: Development of a new correction scheme based on analysis of a global ocean database, *Deep-Sea Res. I,* 57(6), 812-834, doi:10.1016/j.dsr.2010.03.011.

Gouretski, V., 2012: Using GEBCO digital bathymetry to infer depth biases in the XBT data, *Deep-Sea Res. I,* 62, 40-52, doi:10.1016/j.dsr.2011.12.012.

Green A. W., 1984: Bulk dynamics of the expendable bathythermograph (XBT), *Deep-Sea Res*., 31, 415–483.

Hallock, Z., and W. Teague, 1992: The fall rate of T-7 XBT, *J. Atmos. and Ocean. Tech.*, 9, 470-483.

Hamon, M., P. Y. Le Traon, and G. Reverdin, 2011: Empirical correction of XBT fall rate and its impact on heat content analysis. *Ocean Sci. Discuss*., 8, 291–320, doi:10.5194/osd-8-291-2011.

Hanawa, K., P. Raul, R. Bailey, A. Sy, and M. Szabados, 1994: Calculation of new depth equations for expendable bathythermographs using a temperature-error-free method (Application to Sippican/TSK T-7, T-6 and T-4 XBTs), *Tech. Pap. Mar. Sci.*, 67, 46 pp., UNESCO, Paris.

Hanawa, K., P. Raul, R. Bailey, A. Sy, and M. Szabados, 1995: A new depth-time equation for Sippican or TSK T-7, T-6 and T-4 expendable bathythermographs (XBT), *Deep-Sea Res. I*, *42*, 1423-1451.

Hanawa, K, and H. Yoritaka, 1987: Detection of systematic errors in XBT data and their correction, *J. Oceanogr. Soc. of Japan*, 43 (1), 68-76.

Hanawa, K., and T. Yasuda, 1992: New detection method for XBT error and relationship between the depth error and coefficients in the depth-time equation, *J. Oceanogr*., 48, 221-230.

Heinmiller, R. H., C. C. Ebbesmeyer, B. A. Taft, D. B. Olson, and O. P. Nikitin, 1983: Systematic errors in expendable bathythermograph (XBT) profiles, *Deep-Sea Res*., 30(11A), 1185–1197.

Ishii, M., and M. Kimoto, 2009: Reevaluation of historical ocean heat content variations with time-varying XBT and MBT depth bias corrections, *J. Oceanogr*., 65 (3), 287-299.

Kizu, S., and K. Hanawa, 2002: Recorder-dependent temperature error of expendable bathythermograph, *J. Oceanogr.*, *58*, 469-476.

Locarnini, R. A., A. V. Mishonov, J. I. Antonov, T. P. Boyer, H. E. Garcia, O. K. Baranova, M. M. Zweng, and D. R. Johnson, 2010: *World Ocean Atlas 2009*, Volume 1: Temperature. S. Levitus, Ed., NOAA Atlas NESDIS 68, U.S. Government Printing Office, Washington, D.C., 184 pp.

Levitus, S., J. I. Antonov, T. P. Boyer, R. A. Locarnini, H. E. Garcia, and A. V. Mishonov, 2009: Global ocean heat content 1955–2008 in light of recently revealed instrumentation problems, *Geophys. Res. Lett*., 36, L07608, doi:10.1029/2008GL037155.

Olson, R., R. Sriver, M. Goes, N. M. Urban, H. D. Matthews, M. Haran, and K. Keller, 2012: A climate sensitivity estimate using Bayesian fusion of instrumental observations and an Earth system model, *J. Geophys. Res*., 117, D04103, doi:10.1029/2011JD016620.

Reseghetti, F., M. Borghini, and G. M. R. Manzella, 2007: Factors affecting the quality of XBT data – results of analyses on profiles from the Western Mediterranean Sea., *Ocean Sci*., 3, 59-75.

Saunders, P. M., 1981: Practical conversion of pressure to depth, *J. Phys. Oceanogr*., 11, 573-574.

Seaver, G., and S. Kuleshov, 1982: Experimental and analytical error of the expendable bathythermograph, *J. Phys. Oceanogr*., 12, 592-600.

Storn, R., and K. Price, 1997: Differential Evolution - a simple and efficient heuristic for global optimization over continuous spaces, *J. Global Optimization*, Kluwer Academic Publishers, 11, pp. 341 - 359.

Thadathil, P., A. K. Saran, V. V. Gopalakrishna, P. Vethamony, N. Araligidad, and R. Bailey, 2002: XBT fall rate in waters of extreme temperature: A case study in the Antarctic Ocean, *J. Atmos. and Ocean. Tech*., 19, 391-396.

Urban, N., and K. Keller, 2009: Complementary observational constraints in climate sensitivity, *Geophys. Res. Lett*., 36, L04708, doi:10.1029/2008GL036457.

Wijffels, S. E., J. Willis, C. M. Domingues, P. Barker, N. J. White, A. Gronell, K. Ridgway, and J. A. Church, 2008: Changing expendable bathythermograph fall-rates and their impact on estimates of thermosteric sea level rise, *J. Climate*, 21, 5657–626 5672.

List of figures:

Figure 1: Upper panel: Global upper ocean (0-700 m) heat content anomaly (OHCA) as a function of angle (in radians) for one cycle of simulated sinusoidal depth linear biases with amplitude of 2% of depth, based on the WOA09 annual climatology dataset. Lower panels: respective depth bias (Δz) located at the each circle of the angle space in the upper panel. In this illustration, OHCA is the average of 30 realizations which 50% of the world ocean temperature profiles are randomly selected to include the depth biases, therefore simulating the percentage of XBT observations in the World Ocean Database (WOD) during 1967-2001.

Figure 2: Schematic of the pressure switch correction. During the descent of the probe (probe not to scale), a temperature profile is produced. Pressure switches installed in the probe are triggered at various depths, and the recorded measurements P_1, P_2, …, P_n correct the profile to the CTD depth.

Figure 3: Histogram of the error parameters (a) T_0, (b) z_d and (c) z_0, reproduced after correction of one XBT profile. Colored lines represent the corrections with different number of pressure switches applied, n = 1, 2, 3, 4 and 5 respectively. The gray dashed lines are the input errors introduced in the simulated XBT profile that are being estimated.

Figure 4: a) Temperature profiles for CTD (blue circles), XBT (green line with crosses), and corrected XBT profiles that minimize the RMSE using one (n=1; black line), two (n=2; red line), and three (n=3; cyan line) switches. b) Temperature and c) depth differences from the CTD for the XBT (green), n=1 (black), n=2 (red), and n=3 (cyan); d) Median RMSE (m) of the clustered 12,500 random realizations as a function of the depth of the deepest switch for n=1 (black), n=2

(red), and *n*=3 (cyan); and e) box-whisker plots showing the 0, 5, 25, 50, 75, 95 and 100 percentiles of RMSE (m) distribution for all 12,500 realizations for the XBT (*n*=0) and *n*=1 to 5 pressure switches. The XBT profile is simulated using the parameters (z_d, ε_T, ε_Z, ε_p).

Figure 5: Same as Figure 4 but for errors (z_0, z_d, ε_T, ε_Z, ε_p).

Figure 6: Same as Figure 4 but for errors (z_0, T_0, z_d, z_2, ε_T, ε_Z, ε_p).

Figure 7: Median depth RMSE (m) of 12,500 random realizations of the pressure switches positions as a function of the error in the pressure measurement (y-axis) and the number of pressure switches (x-axis). The error in the pressure measurement (E_p) is defined as $E_p = p_0 + \varepsilon_p$, where $\varepsilon_p = N(0,\sigma_p^2)$ as described in equation (14). The error space is sampled in intervals of $\Delta p_0 = 0.2$ m.

Figure 8: Differences between collocated temperature profiles from the PNE 2009 cruise. (a), (c), and (e) are the temperature differences ($T_{xbt} – T_{ctd}$) in °C and (b), (d), and (f) are depth differences in meters. Gray dots are for the original XBT profiles and colored dots for the corrected XBT profiles using one (red), two (blue) and three (green) pressure switches. The dashed black lines represent the confidence intervals given by Sippican (0.2°C for temperature errors, and 5 m or 2% depth, whichever is greater, for depth errors).

Figure 9: Box-whisker plots showing the 5,25,50,75 and 95 percentiles of the error parameter distributions (a) z_0, (b) z_d, (c) T_0, (d) σ_T, (e) $Z(P_n)$, and (f) depth RMSE, for one (red), two (blue) and three (green) switches. In panel (e) the locations of each of the switches are shown as stacked distributions. Panel (f) also shows the depth RMSE for the uncorrected XBT (black).

Figures:

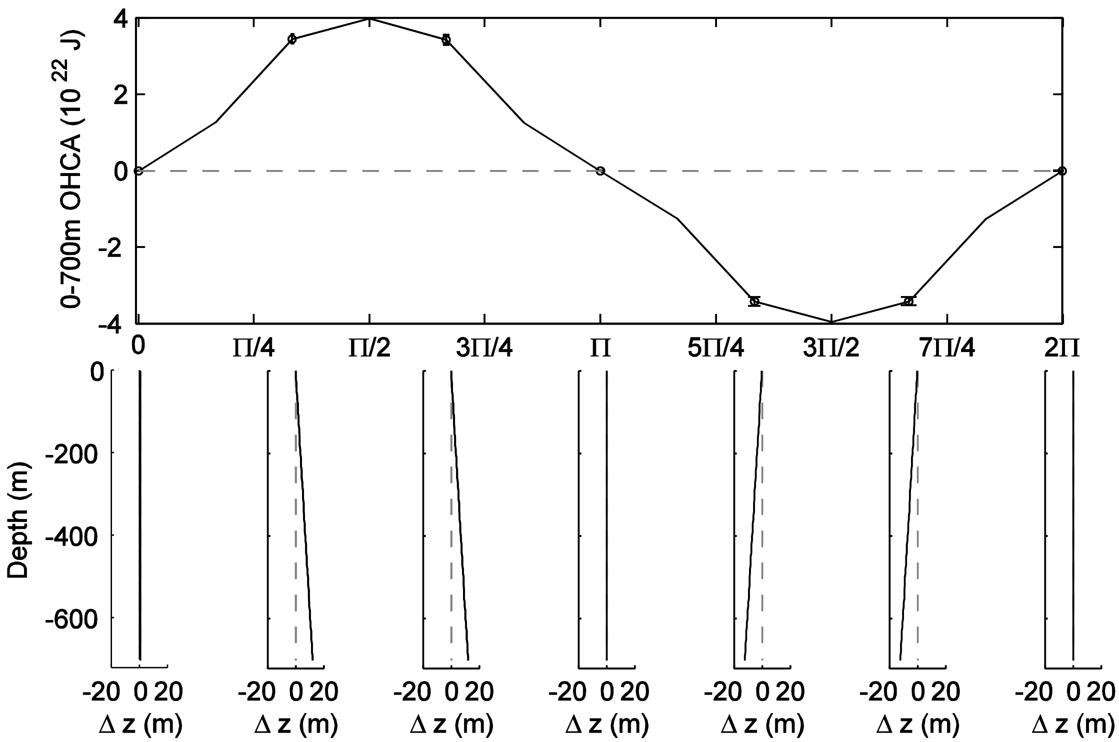

Figure 1: Upper panel: Global upper ocean (0-700 m) heat content anomaly (OHCA) as a function of angle (in radians) for one cycle of simulated sinusoidal depth linear biases with amplitude of 2% of depth, based on the WOA09 annual climatology dataset. Lower panels: respective depth bias (Δz) located at the each circle of the angle space in the upper panel. In this illustration, OHCA is the average of 30 realizations which 50% of the world ocean temperature profiles are randomly selected to include the depth biases, therefore simulating the percentage of XBT observations in the World Ocean Database (WOD) during 1967-2001.

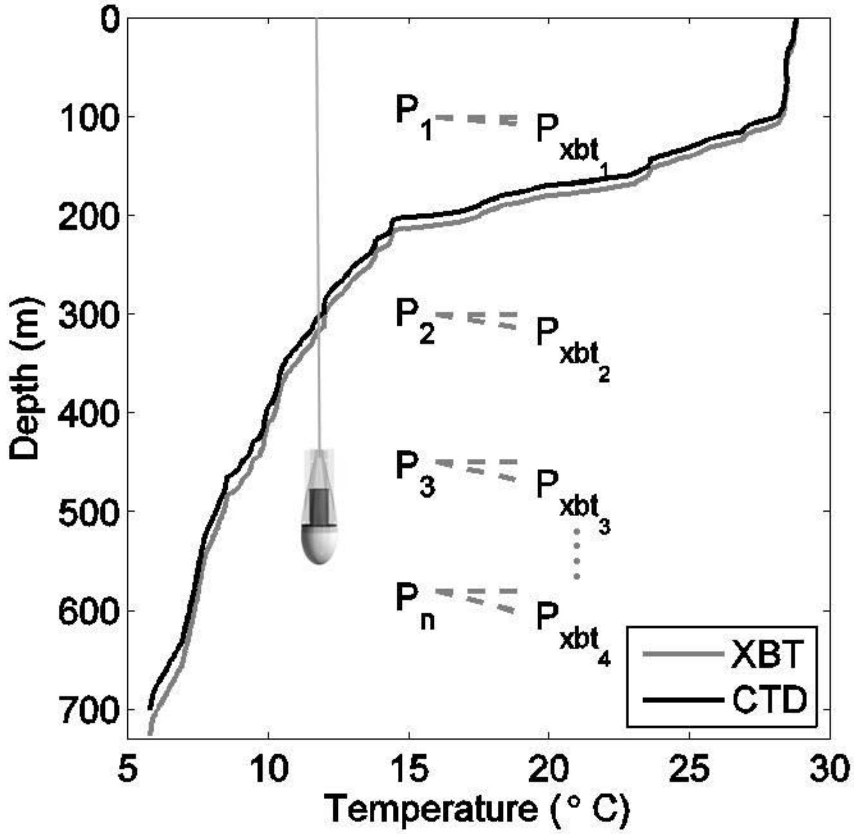

Figure 2: Schematic of the pressure switch correction. During the descent of the probe (probe not to scale), a temperature profile is produced. Pressure switches installed in the probe are triggered at various depths, and the recorded measurements P_1, P_2, …, P_n correct the profile to the CTD depth.

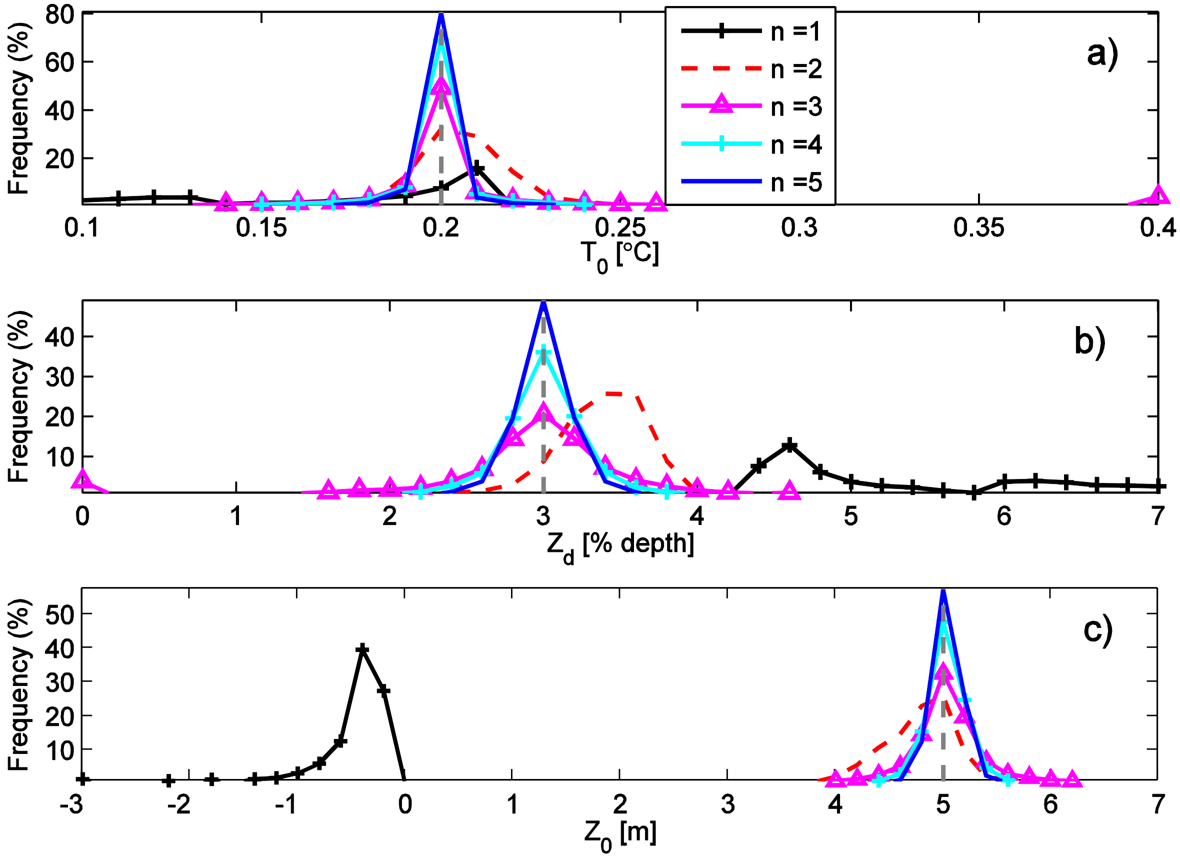

Figure 3: Histogram of the error parameters (a) T_0, (b) z_d and (c) z_0, reproduced after correction of one XBT profile. Colored lines represent the corrections with different number of pressure switches applied, *n* = 1, 2, 3, 4 and 5 respectively. The gray dashed lines are the input errors introduced in the simulated XBT profile that are being estimated.

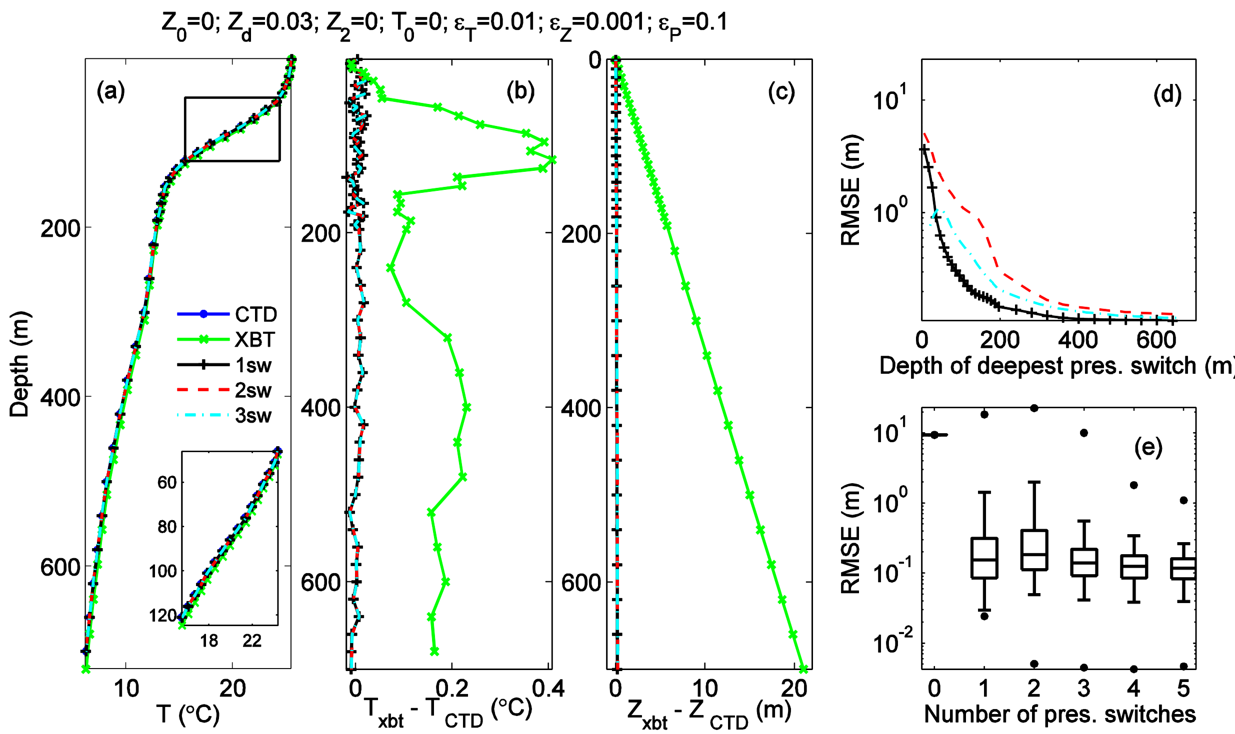

Figure 4: a) Temperature profiles for CTD (blue circles), XBT (green line with crosses), and corrected XBT profiles that minimize the RMSE using one (*n*=1; black line), two (*n*=2; red line), and three (*n*=3; cyan line) switches. b) Temperature and c) depth differences from the CTD for the XBT (green), *n*=1 (black), *n*=2 (red), and *n*=3 (cyan); d) Median RMSE (m) of the clustered 12,500 random realizations as a function of the depth of the deepest switch for *n*=1 (black), *n*=2 (red), and *n*=3 (cyan); and e) box-whisker plots showing the 0, 5, 25, 50, 75, 95 and 100 percentiles of RMSE (m) distribution for all 12,500 realizations for the XBT (*n*=0) and *n*=1 to 5 pressure switches. The XBT profile is simulated using the parameters (z_d, ε_T, ε_Z, ε_p).

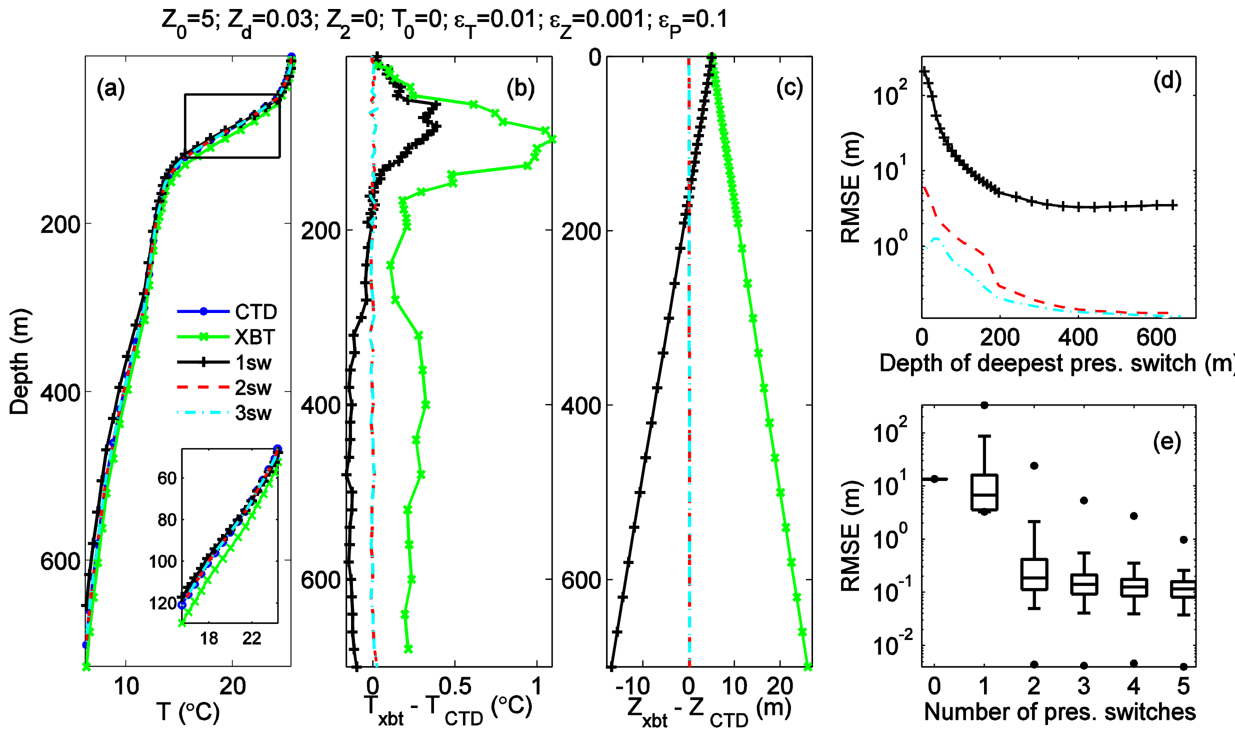

Figure 5: Same as Figure 4 but for errors (z_0, z_d, ε_T, ε_Z, ε_p).

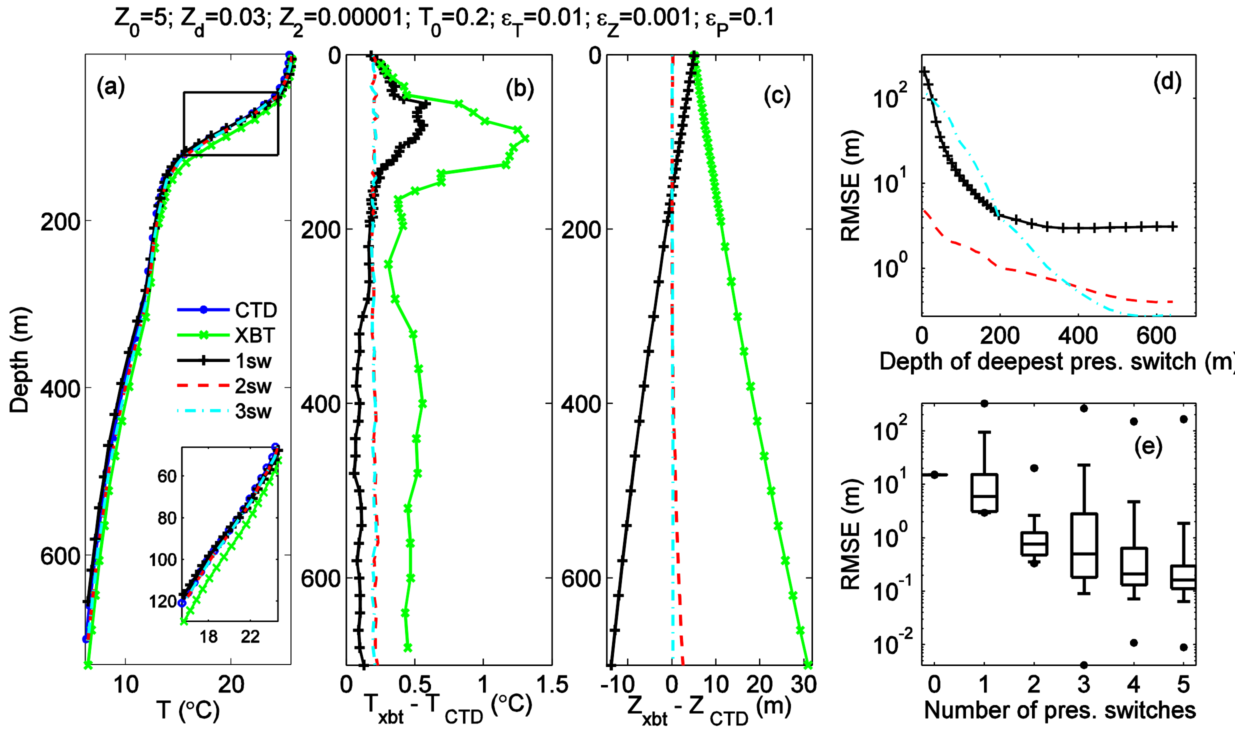

Figure 6: Same as Figure 4 but for errors (z_0, T_0, z_d, z_2, ε_T, ε_Z, ε_p).

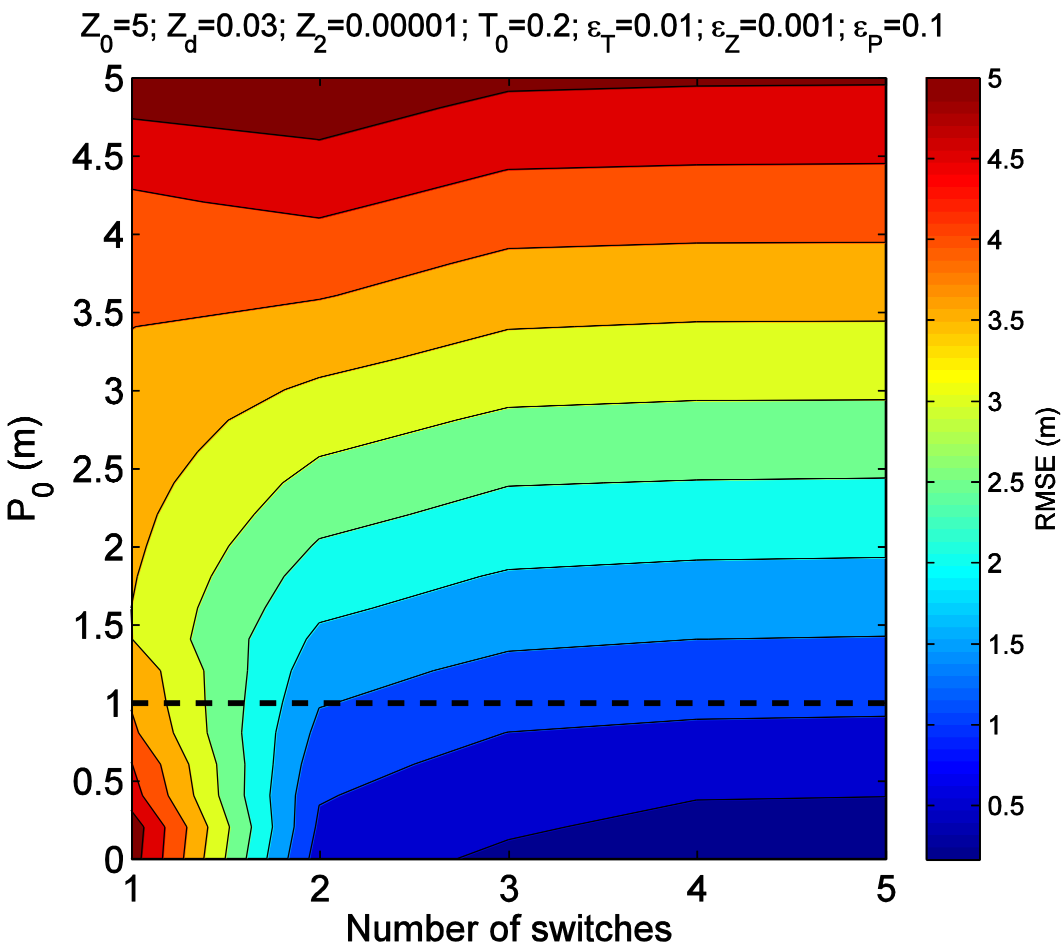

Figure 7: Median depth RMSE (m) of 12,500 random realizations of the pressure switches positions as a function of the error in the pressure measurement (y-axis) and the number of pressure switches (x-axis). The error in the pressure measurement (E_p) is defined as $E_p = p_0 + \varepsilon_p$, where $\varepsilon_p = N(0,\sigma_p^2)$ as described in equation (14). The error space is sampled in intervals of Δp_0 = 0.2 m.

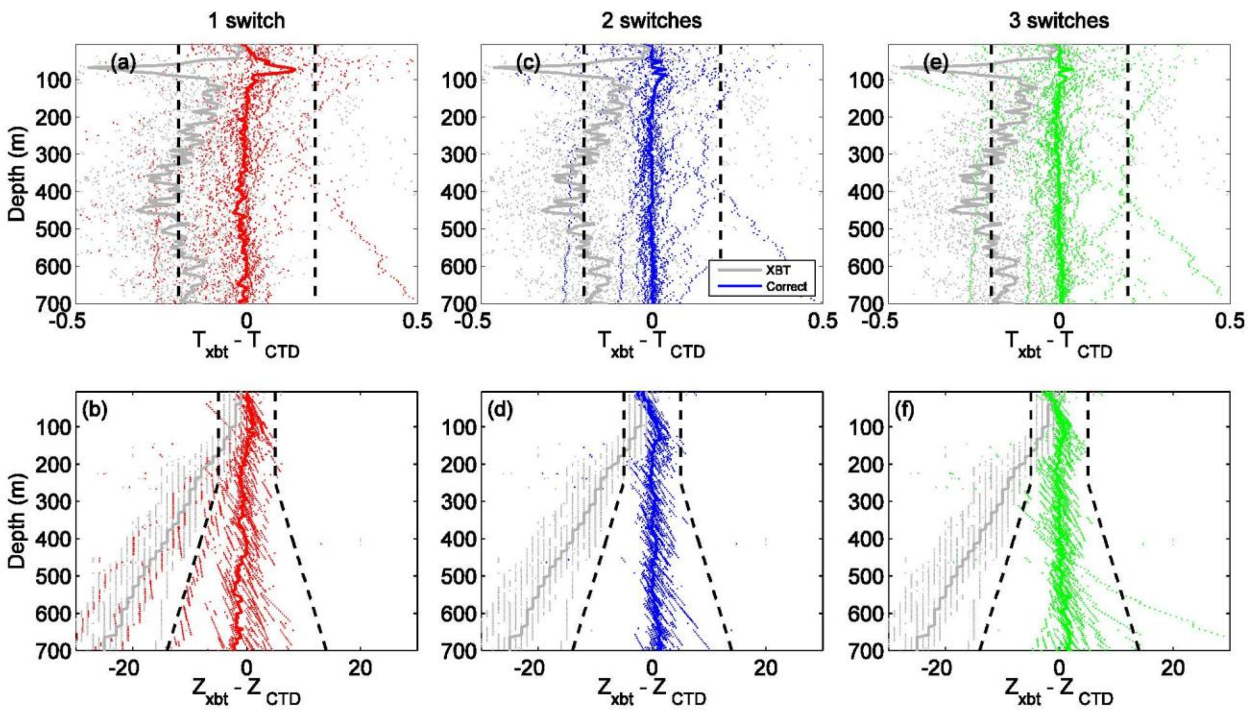

Figure 8: Differences between collocated temperature profiles from the PNE 2009 cruise. (a), (c), and (e) are the temperature differences ($T_{xbt} – T_{ctd}$) in °C and (b), (d), and (f) are depth differences in meters. Gray dots are for the original XBT profiles and colored dots for the corrected XBT profiles using one (red), two (blue) and three (green) pressure switches. The dashed black lines represent the confidence intervals given by Sippican (0.2°C for temperature errors, and 5 m or 2% depth, whichever is greater, for depth errors).

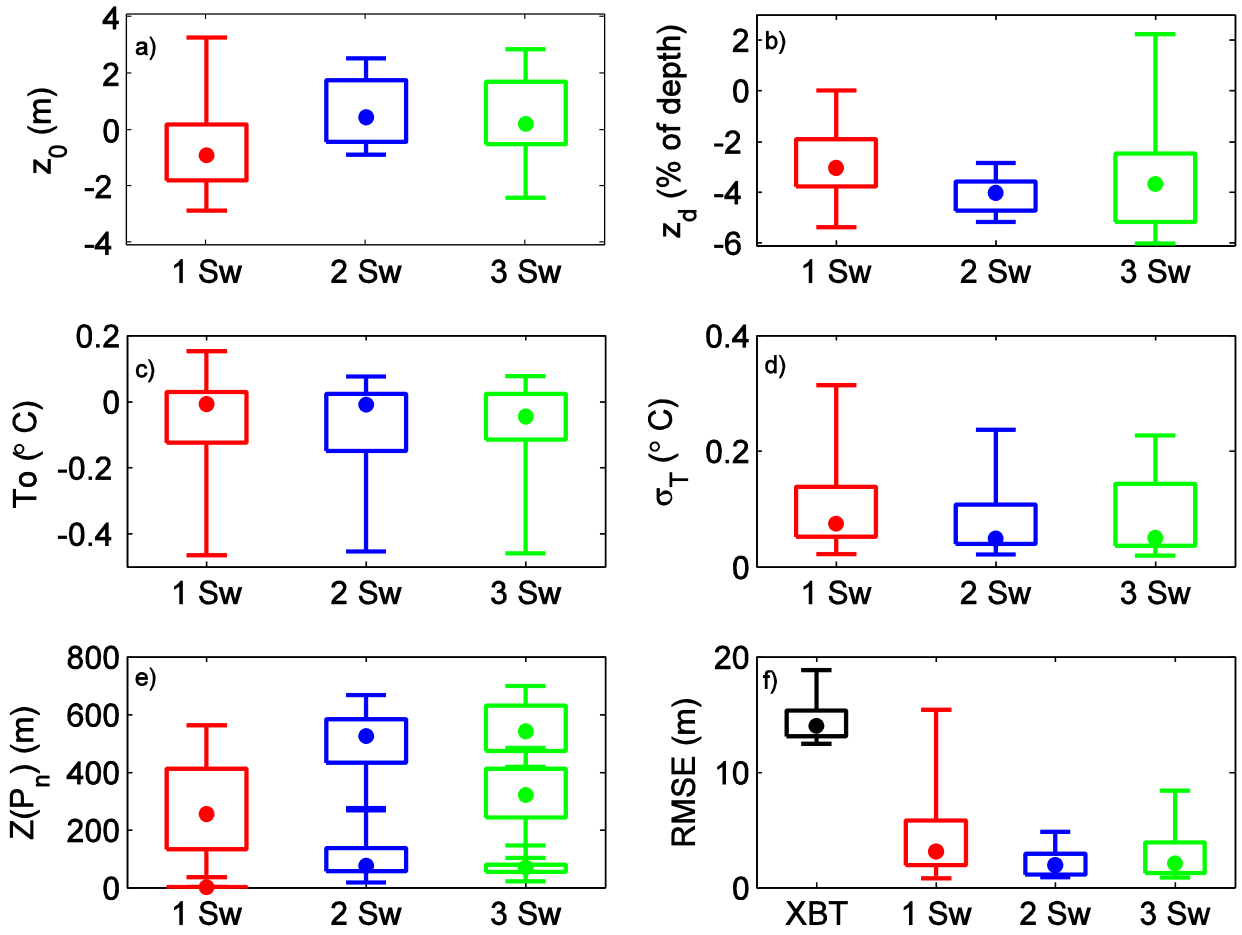

Figure 9: Box-whisker plots showing the 5,25,50,75 and 95 percentiles of the error parameter distributions (a) z_0, (b) z_d, (c) T_0, (d) σ_T, (e) $Z(P_n)$, and (f) depth RMSE, for one (red), two (blue) and three (green) switches. In panel (e) the locations of each of the switches are shown as stacked distributions. Panel (f) also shows the depth RMSE for the uncorrected XBT (black).

Table 1: Error parameter values in the XBT measurements used in this study.

Parameter	**Symbol**	**Typical values**
Thermal offset	T_0	0.2 °C
Depth offset	z_0	5 m
Linear depth bias	z_d	3% of depth
Quadratic depth bias	z_2	$1e^{-5}$ m^{-1}
Depth precision	ε_Z	0.001 m
Temperature precision	ε_T	0.01 °C
Pressure measurement error	ε_p	0.1 dbar (or m)

Table 2: Bootstrapped median and standard deviation of the parameters values optimized for the 19 collocated CTD/XBT profiles, summarizing the results in Figure 9. The parameters are listed in the first column. The second to fourth columns are for the correction using one, two and three pressure switches. The fifth column shows the medians and standard deviations of the parameter values estimated by Dinezio and Goni, 2011 (DG11), when estimates are available.

n	1	2	3	DG11
σ_T (˚C)	0.08±0.07	0.06±0.07	0.05±0.07	--
T_0 (˚C)	-0.001±0.166	-0.01±0.15	-0.04±0.15	-0.03±0.17
z_0 (m)	-0.82±1.79	0.20±1.21	0.22±1.5	0.20±1.54
z_d (%)	-3.48±1.1	-3.96±0.66	3.67±2.3	-3.77±0.57
z_2 (m^{-1})	--	--	$-0.49e^{-5} \pm 4.3e^{-5}$	--
$Z(P_1)$ (m)	0	76±78	69±31	--
$Z(P_2)$ (m)	289± 198	593±168	320±113	--
$Z(P_3)$ (m)	--	--	542±87	--
RMSE	3.1 ± 4.3	1.9±1.3	2.1±2.3	--